

Published in final edited form as:

Biochemistry. 2005 July 19; 44(28): 9574-9580. doi:10.1021/bi0505924.

Crystal Structure of Botulinum Neurotoxin Type G Light Chain -Serotype Divergence in Substrate Recognition, †,‡

Joseph W. Arndt[§]. Wayne Yu[§]. Fay Bi^{§,¶}. and Raymond C. Stevens^{*,§}

§Department of Molecular Biology, The Scripps Research Institute, 10550 N. Torrey Pines Road, La Jolla, CA 92037.

Abstract

The seven serotypes (A–G) of botulinum neurotoxins (BoNTs) block neurotransmitter release through their specific proteolysis of one of the three proteins of the soluble N-ethylmaleimidesensitive-factor attachment protein receptor (SNARE) complex. BoNTs have stringent substrate specificities that are unique for metalloprotease in that they require exceptionally long substrates (1). In order to understand the molecular reasons for the unique specificities of the BoNTs, we determined the crystal structure of the catalytic light chain (LC) of Clostridium botulinum neurotoxin type G (BoNT/G-LC) at 2.35 Å resolution. The structure of BoNT/G-LC reveals a C-terminal βsheet that is critical for LC oligomerization and is unlike that seen in the other LC structures. Its structural comparison with thermolysin and the available pool of LC structures reveals important serotype differences that are likely to be involved in substrate recognition of the P1' residue. In addition, structural and sequence analysis have identified a potential exosite of BoNT/G-LC that recognizes a SNARE recognition motif of VAMP.

Keywords

neurotoxin; light chain; SNARE recognition; S1' subsite; SSR exosite

Botulinum neurotoxins (BoNTs)¹ types A-G cause the paralytic disease known as botulism by preventing neurotransmitter release through the specific cleavage of proteins of the neuorocytosis apparatus known as the soluble N-ethylmaleimide-sensitive-factor attachment protein receptor (SNARE). The causative agent of the toxicity is a 150 kDa multi-domain protein that is processed by endogenous proteases into a 50 kDa light chain (LC) and a 100 kDa heavy chain (HC) that tightly associate via an inter-chain disulfide bond and extensive non-covalent interactions (2,3). The HC has two functional domains that facilitate selective binding to the neuronal presynaptic membrane and translocation of the LC following receptor

[†]This work was supported by contract DAMD17-00-C-0040 from the Department of the Army. Portions of this research were carried out at the General Medicine and Cancer Institutes Collaborative Access Team (GM/CA-CAT) beamlines of the Advanced Photon Source (APS). GM/CA CAT has been funded in whole or in part with Federal funds from the National Cancer Institute (Y1-CO-1020) and the National Institute of General Medical Sciences (Y1-GM-1104). Use of the APS was supported by the U.S. Department of Energy, Basic Energy Sciences, Office of Science, under contract No. W-31-109-ENG-38.

[‡]The coordinates for the structure have been deposited with the Protein Data Bank as entry 1ZB7.

^{*}To whom correspondence should be addressed. Fax: (858)784-9483. E-mail: stevens@scripps.edu. ¶Currently at Princeton University.

 $^{^1}$ Abbreviations. BoNT, botulinum neurotoxin; CV, column volumes; DTT, dithiolthreitol; HC, heavy chain; IPTG, isopropyl α thiogalactopyranoside; LC, light chain; SNAP-25, synaptosomal-associated 25 kDa protein; SNARE, soluble N-ethylmaleimidesensitive-factor attachment protein receptor; SSR, SNARE secondary recognition; TCEP, Tris(2-carboxyethyl)phosphine hydrochloride; TeNT, tetanus neurotoxin; TSA, transition state analog; VAMP, vesicle-associated membrane protein.

mediated endocytosis into the cytosol. The LC is a zinc-metalloprotease that contains all the molecular components for substrate recognition and proteolysis.

BoNT-LCs share significant sequence similarity ranging from 31 – 61 % identity (4), yet each has exclusive substrate specificity. BoNT/A and /E cleave the synaptosomal-associated 25 kDa protein (SNAP-25); BoNT/B, /D, /F, and /G cleave the vesicle-associated membrane protein (VAMP), which is also referred to as synaptobrevin. BoNT/C is broader in its specificity and can cleave both SNAP-25 and synataxin. BoNT-LCs are highly specific for their substrates, but allow amino acid substitutions near the site of peptide bond cleavage with the exception of the amino acid adjacent to the scissile bond on the C-terminal side (P1' position) (5–7). The high specificity of BoNTs has been attributed to additional substrate recognition sites that are remote from the catalytic active site that were identified in the crystal complex structures of BoNT/B-LC with VAMP (8) and BoNT/A1-LC with SNAP-25 (9), as well as SNARE secondary recognition (SSR) sites identified by mutagenesis studies (10–12).

If we are to understand the molecular basis for the unique specificities of BoNTs, it is essential to expose the differences in their structures that give rise to their unique characteristic. Therefore, structures of all serotypes are required, and toward achieving this goal we have determined the crystal structure of *Clostridium botulinum* neurotoxin type G LC (BoNT/G-LC) to 2.35 Å resolution. Comparison of BoNT/G-LC with the available neurotoxin structures reveals subtle yet distinct serotype variations that likely influence LC oligomerization and substrate recognition. This structure helps elucidate the complete function of BoNT/G, as well as complements the structure collection of BoNT-LCs (serotypes A, B, and E) that is known.

EXPERIMENTAL PROCEDURES

Protein production and crystallization of BoNT/G-LC

Overexpression of BoNT/G-LC was induced in the presence of 1 mM ZnCl₂ with isopropyl α-thiogalactopyranoside (IPTG) under control of the T5 promoter in plasmid pBN13, which encodes an expression and purification tag consisting of APPTPGHHHHHH at the C-terminus of the LC protein. Bacteria were lysed by sonication in lysis buffer (50 mM K₂HPO₄ pH 7.8, 300 mM NaCl, 10% glycerol, 5 mM imidazole) supplemented with Roche EDTA-free protease inhibitor tablets and 0.5 mg/ml lysozyme. In addition, 0.25 mM Tris (2-carboxyethyl) phosphine hydrochloride (TCEP) was added throughout the purification. Immediately after sonication, the cell debris was pelleted by ultracentrifugation. The soluble fraction was applied to a gravity flow metal chelation column (Talon resin charged with cobalt; Clontech) equilibrated in lysis buffer. The column was then washed with wash buffer (25 mM Tris pH 7.8, 300 mM NaCl, 10% glycerol, 10 mM imidazole) and eluted with 3 column volumes (CV) of elution buffer (25 mM Tris 7.8, 15 mM NaCl, 150 mM imidazole). The protein was then applied to a Poros 20 HQ column (Applied Biosystems) equilibrated in anion exchange buffer (25 mM Tris pH 7.8). The column was washed with equilibration buffer and eluted with 10 CV gradient elution (0-500 mM NaCl in 25 mM Tris pH 7.8). The protein was then concentrated to ~10 mg/ml by centrifugal ultrafiltration (Orbital), applied to a sizing column (Biocep SEC-S 3000, Phenomenex) equilibrated in size exclusion buffer (150 mM NaCl in 25 mM Tris pH 7.4), and eluted. The purified protein was concentrated to 13 mg/ml (Orbital) and either frozen in liquid nitrogen for later use or used immediately for crystallization trials. The protein was crystallized using the nanodroplet vapor diffusion method (13) at a temperature of 293K. The crystallization solution contained 6% PEG 6000, 0.65 M LiCl, and 100 mM sodium citrate at pH 5.5.

Activity Assay

BoNT solid-phase activity assay optimized for BoNT serotype B was performed with substrate coated plate immobilized with a fluorescene derivatized VAMP peptide (residues 60–94) as described (14). Briefly, assays were conducted in triplicate in 50 mM Hepes at pH 7.4, 1 mM DTT, 0.25 mM ZnCl₂, and 0.05% Tween-20 with 90 μ g/ml BoNT/G-LC and 1 μ g/ml BoNT/B-LC as a positive control. Reactions were incubated on a substrate immobilized plate at 37° C for 5 hr. Fluorescence of the cleavage reaction was measured with a GENios Pro fluoremeter (Tecan) with excitation and emission wavelengths of 485 nm and 535 nm, respectively (Supplemental Figure S1).

Data Collection

Diffraction data were collected at the Advanced Photon Source (APS, Argonne, USA) on beamline GM/CA CAT-23ID at a wavelength of 1.009 Å using the MAR data collection environment (Table 1). The data sets were collected at 100K using a MAR 225 CCD detector. Data were integrated, reduced, and scaled using HKL2000 (15). The crystals were indexed in the hexagonal space group P622; data statistics are summarized in Table 1.

Structure Determination and Refinement

The structure was determined by with MOLREP (16) using the two possible space groups, P6₂22 and P6₄22, predicted from the observed systematic absences. Only the P6₂22 space group yielded the correct solution. ARP/wARP (17) was used to build 94% of the model followed by manual building of the rest of the structure with O (18). Structure refinement was performed using REFMAC5 (19). Refinement statistics are summarized in Table 1. The final model includes a single protein molecule, a citrate molecule in coordination to the active site zinc ion, and 198 water molecules. No electron density was observed for residues 53–67, 211–213, 252–256, and 439–445. Analysis of the stereochemical quality of the model was accomplished using the AutoDepInputTool (http://deposit.pdb.org/adit/). Figures were prepared with PyMOL (DeLano Scientific). Atomic coordinates and experimental structure factors of BoNT/G-LC have been deposited with the PDB and are accessible under the code 1ZB7.

Substrate Modeling

The potential S1' binding subsite of BoNT/G-LC, as well as the other LC serotypes, for recognition of the P1' residue was identified by comparing the structure of BoNT/G-LC with that of metalloprotease thermolysin (PDB code 4TMN) (20) bound to a transition state analog (TSA). The modeling strategy involved superimposing the active site HExxH motif of this protein with that of BoNT/G-LC using the web server C-alpha Match (http://bioinfo3d.cs.tau.ac.il/c_alpha_match/).

The probable SSR site of BoNT/G-LC that is specific for the V2 SSR of VAMP was identified by comparison of BoNT/G-LC with the structure of the mutant E224Q/Y366F of BoNT/A1-LC in complex with residues 141–204 of SNAP-25 (PDB code 1XTG) (9) with the program TOP (21). A five residue region containing the three essential acidic residues of V2 SSR motif of VAMP (residues 64-68) were modeled to BoNT/G-LC based on the analogous residues in SNAP-25 (residues 180-184) that are 14 residues upstream from the proteolytic cleavage site.

RESULTS AND DISCUSSION

Structure of BoNT/G-LC

The structure of BoNT/G-LC (Figure 1A) was determined to 2.35 Å resolution by molecular replacement using the BoNT/B-LC structure (PDB code 1F82 (8) with 61% sequence identity) as the search model. Data collection, model, and refinement statistics are summarized in Table 1. The final model of the BoNT/G-LC structure is composed of fourteen β -strands ($\beta 1 - \beta 14$), eight α -helices ($\alpha 1 - \alpha 8$), and four 3_{10} -helical segments ($\eta 1 - \eta 4$) that form a homodimer through crystallographic symmetry. Homodimeric structures are also found in the LC structures of BoNT/A2 (22) and /E (23), suggesting a potential importance of LC oligomerization. The dimensions of the BoNT/G-LC homodimer are 115 Å \times 56 Å \times 38 Å, with an overall surface area of 27,800 Å². The overall conformation of the BoNT/G-LC monomer is similar to the LC structures of BoNT/A1 (9), /A2 (22), /B (8), and /E (23) with minor differences observed for the loop regions (25, 145, 200, 250, and 310 loops). However, two distinguishing features set it apart from the other LC structures, those being an extra βsheet and a channel that connects the two active sites of the homodimer. The additional antiparallel β-sheet is located near the C-terminus and is composed of β-strands β4 (residues 69– 73) and β14 (residues 429–436) (Figure 1A). This region is directly before the inter-chain disulfide bond and contributes to the dimerization interface. A similar β-sheet is seen in the catalytic domain of BoNT/B holotoxin (2) between β-strands β4 (residues 71–72) and β20 (residues 429–430), though the β -sheet in the BoNT/G-LC structure is more extensive. Consistent with this observation, DasGupta reported that the single chain holotoxin significantly alters its structure upon nicking as observed in the increase in the prevalence of β-sheet from 37 to 41% (24). The BoNT/A1, /A2, and /B-LC structures lack this secondary structure element, likely because they are C-terminal truncated variants and not full length LCs (Table 2).

The second structural feature unique to BoNT/G-LC is that the active sites are connected via a serpentine-like channel (Figure 1B) that is partially covered but not blocked by β -strand β 14 and terminal residues of the C-terminus (residues 437–438) of each subunit (Figure 1A). The individual active sites of the BoNT/G-LC homodimer are solvent accessible and joined by a contiguous channel 28.5 Å in length. The channel takes an abrupt 90° turn at each of the active sites of the homodimer where it continues another ~17 Å along the groove primarily formed by the 175 and 250 loops. Intriguing as it may be, to our knowledge there is no evidence that suggests that these active sites work in a cooperative manner. Thus, further studies should be conducted to determine if there is a functional significance to the observed channel or if it is merely a packing artifact.

Evidence of the importance of the C-terminus in LC transport and proteolytic activity are increasingly mounting. Fernandez-Salas and colleagues recently reported that the N- and C-termini of BoNT/A and /E-LCs are critical in its localization (25). In particular they showed that mutations and deletions of the C-terminus of BoNT/A-LC suggest that it is likely involved in trafficking and/or interaction with membrane adaptor proteins through a diluccine motif ($\underline{E}^{423}XXX\underline{LL}^{428}$). A dileucine to dialanine mutant (L427A and L428A) revealed that disruption of this motif caused changes in the steady-state distribution of BoNT/A-LC in the plasma membrane resulting in the mutant being distributed in the periplasmalemmal space instead of plasma membrane localized, as well as being 26- fold less active than the wild-type BoNT/A-LC. Moreover, a C-terminal truncated construct of BoNT/A-LC (Δ C22), lacking 22 C-terminal acids, displayed similar altered distribution with ~80 fold decreased activity. Consistent with this observation of reduced catalysis are the reports of ~10 fold decreased activity of C-terminal truncated LC variants of BoNT/A1 Δ C30 and Δ C50 (26) and BoNT/A2 Δ C32 (27), thus further implicating the significance of the LC C-terminus. Incidentally, the Δ C32 BoNT/A2-LC variant is the protein construct used to obtain the crystal structure of

BoNT/A2 while the Δ C22 variant is similar in size to the Δ C18 construct used in the BoNT/A1 structure (Table 2). It is clear from these separate studies that the C-terminus can influence activity. However, it is not yet apparent if different localization motifs are present in the other LC serotypes, since the dileucine motif is unique to BoNT/A, or if the C-terminal β -sheet is common to all BoNT serotypes, since the BoNT/E-LC structure is full length and it is helical in this equivalent position. Thus, further structural studies of other full length BoNT-LCs are needed.

BoNT/G-LC oligomerization

The crystal packing in the BoNT/G-LC structure shows a homodimer, which is non-covalent as determined by SDS-PAGE under non-reducing conditions, and is formed through mostly hydrophobic interactions (69% nonopolar) that associate via a twofold rotation. The dimer interface is composed of β -strands β 10 and β 11, 250 loop, and the C-terminal β -strands β 14 of each subunit, which form an inter-chain anti-parallel β-sheet (Figure 1A). Additional interactions are formed around α -helix α 5 and the 370 loop from each subunit. This intimate dimer interface accounts for a buried surface area of 2054 Å² (10.6% of the total surface area) for each monomer and includes sixteen hydrogen bonds and two salt bridges (R217-D262 from each monomer) as determined by the Protein-Protein Interaction Server (http://www.biochem.ucl.ac.uk/bsm/PP/server/) (28). It is anticipated that the oligomerization state of BoNT/G-LC may be more biologically relevant than those seen in BoNT/A2-LC (22) and BoNT/E-LC (23), since its interface is more hydrophobic and considerably more extensive as indicated by the lower buried surface areas of BoNT/A2- and /E-LCs, 1512 Å² and 1181 Å², respectively (28). Nonetheless, the BoNT/G-LC structure has a similar quaternary structure to BoNT/A2-LC (PDB code 1E1H) (22) with equivalent structural elements forming its dimer interface, with the exception that the 250 loop of each of the subunits of BoNT/A2-LC covers the active site of the homodimer partner. This altered interface results in one of the subunits of BoNT/A2-LC being rotated (~120°) relative to that of the BoNT/G-LC dimer. As a result, BoNT/A2-LC was observed to be auto-proteolytic in solution and crystalline states (22). Analysis of a dissolved crystal of the BoNT/G-LC by SDS-PAGE yielded a single 50 kDa band indicating that the self cleavage observed in the BoNT/A2-LC crystal does not occur in BoNT/G-LC crystal (data not shown). Interestingly, crystal packing shows that the dimeric BoNT/G-LC is covalently linked to another dimer molecule by two inter-chain disulfides to form a homotetramer. The observed dimer-dimer interface is relatively small (1672 Å², 4.8% of the total surface area) (28, 29) and, therefore, may be an artifact of the crystal packing. However, it could also suggest a model of redox dependent oligomeric states like that seen with the EF-hand protein P11 (30), since there is evidence that the tetramer exists in solution, but only under oxidizing conditions, as determined by size exclusion chromatograph. This issue of oligomerization is interesting, since it may be possible that some of the serotypes form higher order oligomeric states in vivo. The differences reported in oligomerization of the LC crystal structures may explain functional variations observed in the serotypes. For instance, the dissimilarity observed in duration of the therapeutic effects in the long-acting BoNT/A compared to the short-acting BoNT/E (25) by influencing the exposure (or protection) of labile regions of the LC, such as epitopes and loops, that are susceptible to immuno-response and proteolytic digestion.

Substrate recognition—Each BoNT serotype is known to require substrates with a minimum length and proper sequence. The unique specificity of each of the serotypes is likely due to the fact that each LC possesses two or more substrate recognition sites as proposed for BoNT/G-LC with its substrate VAMP in Figure 2. The first consists of the subsites located near the active site that are required for discrimination of SNARE residues in proximity to the cleavage site, such as the strictly required P1' substrate residue. The second site, termed exosite, is far removed from the active site and is involved in recognition of the nine residue SSR

sequence motif. Substrate cleavage occurs only when the binding of the SNARE substrate to each of these sites takes place (11,31). Therefore, substrate specificity is likely to be a result of the spatial relationship between an exosite of the LC that recognizes a SSR motif and the active site, which is composed of one or more subsites including, but not necessarily limited to, the S1' subsite for recognition of the essential P1' amino acid on the different SNARE proteins (8,11). Hence, substrate proteolysis only occurs upon binding of the SSR motif that is the proper distance away from the cleavage site.

It has been very challenging to obtain LC-substrate crystal structures and, consequently, the details of substrate recognition are limited and sometimes contradictory. Indeed our attempts at to obtain a cocrystal structure of BoNT/G-LC have yet to be successful. Cocrystal structures of BoNT/A1 (9) and /B-LC (8) reveal that BoNTs bind their substrate SNARE proteins at a channel formerly occupied by 54 residues known as the 'belt' region connecting the LC to the translocation domain, as previously proposed (8). Unfortunately, these structures do not offer insight into the intimate details of substrate recognition of the P1' residue and the SSR motif. The BoNT/A1-LC (E224Q/Y366F double mutant) SNAP-25 complex structure does not allow the mapping of the S1' subsite, since the substrate is disordered in the active site, nor does it reveal any details in the recognition of the conserved residues of the required SSR motif (9). Furthermore, the BoNT/B-LC VAMP complex structure has been the subject of debate (32, 33) due to the low occupancy and atypical orientation of substrate binding as compared to other HExxH proteases. In the absence of a BoNT/G-LC VAMP complex structure, two probable recognition sites of BoNT/G-LC, a S1' subsite and a SSR exosite, are identified based on homology modeling and are discussed individually in the following subsections.

S1' subsite comparison with other serotype LC structures

Despite the unique substrate specificities of the BoNTs, their active sites are highly similar to each other. In BoNT/G-LC the active site zinc is coordinated by His 230 and His 234 of the HExxH motif and Glu 268 of α -helix α 4, as does its counterparts in the other serotypes. However, the high active site residue conservation of BoNTs is not expected to extend to the S1'subsite given the strict dependence for the P1' residues of their SNARE substrates (5–7, 34). The P1' residues are chemically diverse; they vary in size and also range in increasing order of hydrophobicity from Arg (BoNT/A), Lys (BoNT/F), Ala (BoNT/C and /G), Phe (BoNT/B), Leu (BoNT/D), and Ile (BoNT/E) (35). Given the diverse chemical nature of the P1' residues, it is expected that each BoNT serotype would have a complementary S1' subsite for recognition of this structurally varied pool of P1' residues of their SNARE substrates.

Even with the number of different neurotoxin light chain structures now available (serotypes A, B, E, G, and tetanus), surprisingly the S1' subsite of the BoNT-LCs has yet to be convincingly mapped. Here we attempt to define the S1' subsite of BoNT/G-LC by a structural comparison with that of thermolysin, considered to be the prototypical HExxH motif protease, in complex with a TSA containing leucine at the P1' residue. BoNT-LCs show significant structural homology to thermolysin as indicated by the fact that BoNT/G-LC and thermolysin (PDB code 4TMN) (20) can be superposed with a C_{α} RMSD of 2.05 Å for 120 structurally equivalent C_{α} atoms. The superposition reveals the P1' leucine residue of the TSA is directed toward a shallow pocket believed to be the S1' subsite of BoNT/G-LC that is composed of Asn 170, Asn 201, Thr 227, and Tyr 376 (Figure 3A). Importantly, LC structures of BoNT/A1, /B, and /E also have binding cavities at this same location, but their putative S1' subsites are complementary in size and hydrophobicity to their cognate P1' substrate residues (Table 3). The S1' subsite of BoNT/G-LC (Figure 3B) is relatively small and shallow compared to the S1' subsites of the other serotypes (Figure 3C-E) and, therefore, is well suited for the P1' Ala of VAMP. The pocket is made smaller than the S1' subsites of BoNT/A1, /B and /E primarily due to the steric bulk of Tyr 376 that partially fills this cavity. The S1' subsite of BoNT/E-LC

is also small, but deeper and more hydrophobic reflecting the nature of the P1' Ile of SNAP-25 (Figure 3E). In contrast the S1' subsites of BoNT/A1-LC (Figure 3C) and BoNT/B-LC (Figure 3D) are considerably larger than their BoNT/G- and /E-LC counterparts. The BoNT/A1-LC S1' subsite is specific for the P1' Arg of SNAP-25, and likely forms a buried salt bridge with Asp 370 at the bottom of its pocket. The BoNT/B-LC S1' subsite is the largest of the four serotypes investigated, and is well-matched for the P1' Phe of VAMP. Homology modeling reveals the anticipated disparity in the S1' subsites of the different LCs that likely account for their unique P1' specificities, however, additional studies are clearly required to confirm this.

SSR in VAMP specific neurotoxins

It is clear that P1' recognition alone cannot account for the high specificity of BoNTs. Indeed substrate recognition is enhanced by the contribution of high affinity exosites that are far removed from the active site, such as the yet to be identified exosite for binding of the consensus SSR motif found each of the three SNARE proteins (10). The SSR motif is composed of nine residues and contains three conserved acidic residues at positions 3, 4, and 7 (Figure 2). This motif is present in two copies in VAMP, termed V1 (residues 38–47) and V2 (residues 62–71) (10). The essential role of the three conserved acidic residues in this motif in substrate recognition by VAMP specific neurotoxins was demonstrated by mutagenesis of residues comprising this motif. These studies revealed that the V2 copy is critical for recognition by BoNT/B and BoNT/G, while in contrast the V1 is imperative for recognition by tetanus neurotoxin (TeNT) (11), as observed in the dramatic decrease in the rate of proteolysis of mutant VAMP substrates. Our structural and sequence analysis of these VAMP specific neurotoxins helps to reconcile the differences observed in their SSR properties. The BoNT/ BLC VAMP crystal structure identified key residues involved in the recognition of the V2 SSR motif of VAMP. These LC residues include Arg 67, Tyr 72, Asp 375, Ser 376, and Glu 422. The equivalent residues in BoNT/G-LC are only partially conserved (Supplemental Figure S2). Furthermore, a superposition of the two structures (not shown) reveals that this motif clashes with the β -strand β 4 of BoNT/G-LC structure. Therefore, unless there is a conformational rearrangement in this region, it is unlikely that BoNT/G-LC shares the same SSR exosite as that defined in the BoNT/B-LC VAMP structure. However, based on the structural comparison of BoNT/G-LC to BoNT/A-LC SNAP-25 complex structure (PDB code 1XTG, with an overall sequence identity of 31%), Lys 140 and Lys 152 of the BoNT/G-LC are likely to influence the SSR of the V2 carboxylates, presumably by salt bridge formation. An overlay of the BoNT/ G-LC structure with the structure of SNAP-25 from the BoNT/A-LC SNAP-25 complex (9) shows that three basic residues of the BoNT/G-LC, Lys 140, Lys 141, and Lys 152, are in close proximity to the SNAP-25 residues that correspond to the three acidic residues of the V2 SSR of VAMP (Figure 4). An alignment of BoNT/G-LC with the other BoNT and TeNT serotypes and strains reveals that two of these lysine residues, Lys 140 and Lys 152, are also conserved in the BoNT/B strains, which also require the V2 SSR, but not TeNT which does recognize the V2 SSR although is specific for the V1 SSR (Supplemental Figure S2) (11). Further functional and structural studies will be needed to determine if this putative SSR recognition site is correct.

CONCLUSION

The crystal structure of BoNT/G-LC presented complements the structural pool of neurotoxin structures, and in doing so highlights the importance of the C-terminus. The identification of the putative of a S1' subsite is consistent with the available LC structures of BoNT/G, /A, /B, and /E, and thereby provides a molecular basis for the strict specificity for P1' residues of their SNARE protein substrates. A putative SSR site is identified in the BoNT/G-LC structure that is consistent with the biochemical evidence of the importance of this SSR motif in substrate

recognition. Collectively, our structural analysis may lead to development of highly specific inhibitors for BoNT/G and other serotypes.

Supplementary Material

Refer to Web version on PubMed Central for supplementary material.

ACKNOWLEDGMENT

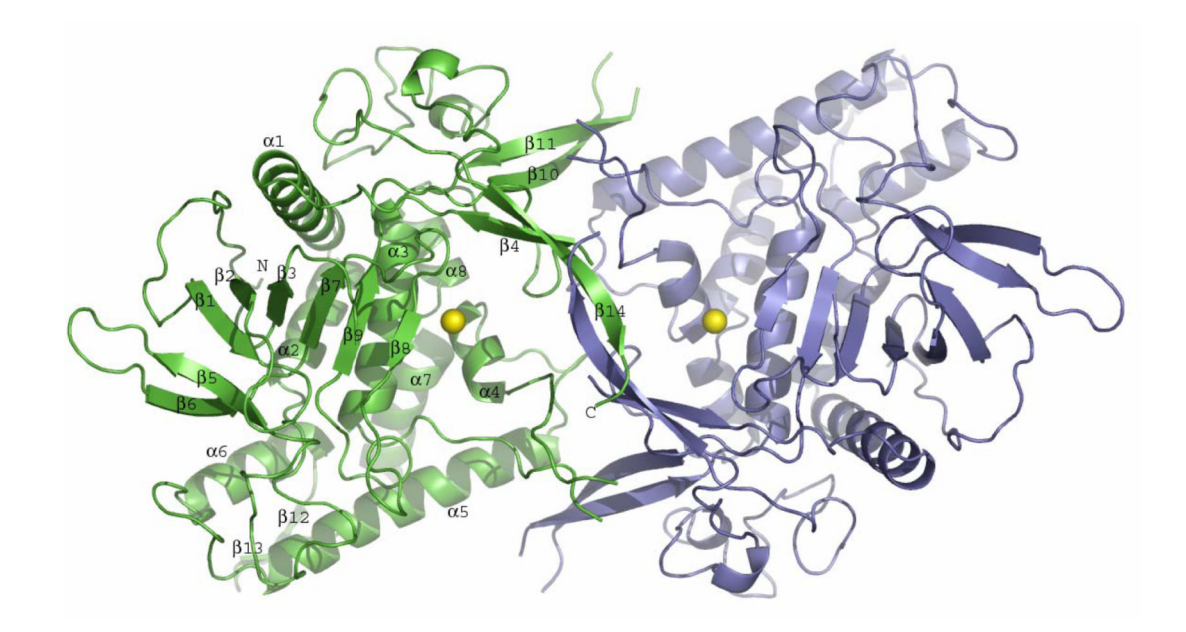
We thank Jim Schmidt for providing the VAMP immobilized plates for the activity assay and Angela Walker for assistance in manuscript preparation.

REFERENCES

- Yamasaki S, Binz T, Hayashi T, Szabo E, Yamasaki N, Eklund M, Jahn R, Niemann H. Botulinum Neurotoxin Type-G Proteolyses the Ala(81)-Ala(82) Bond of Rat Synaptobrevin-2. Biochemical and Biophysical Research Communications 1994;200:829–835. [PubMed: 7910017]
- Swaminathan S, Eswaramoorthy S. Structural analysis of the catalytic and binding sites of Clostridium botulinum neurotoxin B. Nature Structural Biology 2000;7:693–699.
- 3. Lacy DB, Tepp W, Cohen AC, DasGupta BR, Stevens RC. Crystal structure of botulinum neurotoxin type A and implications for toxicity. Nature Structural Biology 1998;5:898–902.
- 4. Thompson JD, Higgins DG, Gibson TJ. Clustal-W Improving the Sensitivity of Progressive Multiple Sequence Alignment through Sequence Weighting, Position-Specific Gap Penalties and Weight Matrix Choice. Nucleic Acids Research 1994;22:4673–4680. [PubMed: 7984417]
- Schmidt JJ, Stafford RG, Bostian KA. Type A botulinum neurotoxin proteolytic activity: development
 of competitive inhibitors and implications for substrate specificity at the S1' binding subsite. FEBS
 Lett 1998;435(1):61–64. [PubMed: 9755859]
- Vaidyanathan VV, Yoshino K, Jahnz M, Dorries C, Bade S, Nauenburg S, Niemann H, Binz T. Proteolysis of SNAP-25 isoforms by botulinum neurotoxin types A, C, and E: Domains and amino acid residues controlling the formation of enzyme-substrate complexes and cleavage. Journal of Neurochemistry 1999;72:327–337. [PubMed: 9886085]
- Schmidt JJ, Stafford RG. Botulinum neurotoxin serotype f: identification of substrate recognition requirements and development of inhibitors with low nanomolar affinity. Biochemistry 2005;44:4067– 4073. [PubMed: 15751983]
- 8. Hanson MA, Stevens RC. Cocrystal structure of synaptobrevin-II bound to botulinum neurotoxin type B at 2.0 angstrom resolution. Nature Structural Biology 2000;7:687–692.
- 9. Breidenbach MA, Brunger AT. Substrate recognition strategy for botulinum neurotoxin serotype A. Nature 2004;432:925–929. [PubMed: 15592454]
- 10. Rossetto O, Schiavo G, Montecucco C, Poulain B, Deloye F, Lozzi L, Shone CC. Snare Motif and Neurotoxins. Nature 1994;372:415–416. [PubMed: 7984234]
- Pellizzari R, Rossetto O, Lozzi L, Giovedi S, Johnson E, Shone CC, Montecucco C. Structural determinants of the specificity for synaptic vesicle-associated membrane protein/synaptobrevin of tetanus and botulinum type B and G neurotoxins. Journal of Biological Chemistry 1996;271:20353– 20358. [PubMed: 8702770]
- 12. Washbourne P, Pellizzari R, Baldini G, Wilson MC, Montecucco C. Botulinum neurotoxin types A and E require the SNARE motif in SNAP-25 for proteolysis. Febs Letters 1997;418:1–5. [PubMed: 9414082]
- 13. Santarsiero B, Yegian D, Lee C, Spraggon G, Gu J, Scheibe D, Uber D, Cornell E, Nordmeyer R, Kolbe W, Jin J, Jones A, Jaklevic J, Schultz P, Stevens R. An approach to rapid protein crystallization using nanodroplets. J. Appl. Crystallogr 2002;35:278–281.
- Schmidt JJ, Stafford RG, Millard CB. High-throughput assays for botulinum neurotoxin proteolytic activity: Serotypes A, B, D, and F. Analytical Biochemistry 2001;296:130–137. [PubMed: 11520041]
- 15. Otwinowski Z, Minor W. Macromolecular Crystallography 1997;Pt A:307-326.

 Vagin A, Teplyakov A. MOLREP: an automated program for molecular replacement. J. Appl. Crystallogr 1997;30:1022–1025.

- 17. Perrakis A, Morris R, Lamzin VS. Automated protein model building combined with iterative structure refinement. Nature Structural Biology 1999;6:458–463.
- Jones TA, Zou JY, Cowan SW, Kjeldgaard M. Improved Methods for Building Protein Models in Electron- Density Maps and the Location of Errors in These Models. Acta Crystallographica 1991;A47:110–119. [PubMed: 2025413]
- 19. Collaborative Computational Project Number 4. The CCP4 Suite: Programs for Protein Crystallography. Acta Crystallogr. 1994;D50:760-763. Acta Crystallogr 1994;D50:760-763.
- Monzingo AF, Matthews BW. Binding of N-Carboxymethyl Dipeptide Inhibitors to Thermolysin Determined by X-Ray Crystallography - a Novel Class of Transition-State Analogs for Zinc Peptidases. Biochemistry 1984;23:5724–5729. [PubMed: 6395881]
- Lu GG. TOP: a new method for protein structure comparisons and similarity searches. J. Appl. Crystallogr 2000;33:176–183.
- 22. Segelke B, Knapp M, Kadkhodayan S, Balhorn R, Rupp B. Crystal structure of Clostridium botulinum neurotoxin protease in a product-bound state: Evidence for noncanonical zinc protease activity. Proceedings of the National Academy of Sciences of the United States of America 2004;101:6888–6893. [PubMed: 15107500]
- 23. Agarwal R, Eswaramoorthy S, Kumaran D, Binz T, Swaminathan S. Structural analysis of botulinum neurotoxin type E catalytic domain and its mutant Glu212 -> Gln reveals the pivotal role of the Glu212 carboxylate in the catalytic pathway. Biochemistry 2004;43:6637–6644. [PubMed: 15157097]
- 24. DasGupta, BR. The Structure of Botulinum Neurotoxins. New York: Marcel Dekker; 1994.
- 25. Fernandez-Salas E, Steward LE, Ho H, Garay PE, Sun SW, Gilmore MA, Ordas JV, Wang J, Francis J, Aoki KR. Plasma membrane localization signals in the light chain of botulinum neurotoxin. Proceedings of the National Academy of Sciences of the United States of America 2004;101:3208–3213. [PubMed: 14982988]
- Baldwin MR, Bradshaw M, Johnson EA, Barbieri JT. The C-terminus of botulinum neurotoxin type A light chain contributes to solubility, catalysis, and stability. Protein Expression and Purification 2004;37:187–195. [PubMed: 15294297]
- 27. Kadkhodayan S, Knapp MS, Schmidt JJ, Fabes SE, Rupp B, Balhorn R. Cloning, expression, and one-step purification of the minimal essential domain of the light chain of botulinum neurotoxin type A. Protein Expression and Purification 2000;19:125–130. [PubMed: 10833399]
- 28. Jones S, Thornton JM. Principles of protein-protein interactions. Proceedings of the National Academy of Sciences of the United States of America 1996;93:13–20. [PubMed: 8552589]
- 29. Henrick K, Thornton JM. PQS: a protein quaternary structure file server. Trends in Biochemical Sciences 1998;23:358–361. [PubMed: 9787643]
- 30. Rety S, Sopkova J, Renouard M, Osterloh D, Gerke V, Tabaries S, Russo-Marie F, Lewit-Bentley A. The crystal structure of a complex of p11 with the annexin II N-terminal peptide. Nature Structural Biology 1999;6:89–95.
- 31. Montecucco C, Schiavo G. Structure and function of tetanus and botulinum neurotoxins. Quarterly Reviews of Biophysics 1995;28:423–472. [PubMed: 8771234]
- 32. Stevens R, Hanson M. Questions about the structure of the botulinum neurotoxin B light chain in complex with a target peptide Response to Rupp and Segelke. Nature Structural Biology 2001;8:664–664.
- 33. Rupp B, Segelke B. Questions about the structure of the botulinum neurotoxin B light chain in complex with a target peptide. Nature Structural Biology 2001;8:663–664.
- 34. Washbourne P, Bortoletto N, Graham ME, Wilson MC, Burgoyne RD, Montecucco C. Botulinum neurotoxin E-insensitive mutants of SNAP-25 fail to bind VAMP but support exocytosis. Journal of Neurochemistry 1999;73:2424–2433. [PubMed: 10582602]
- 35. Schiavo G, Matteoli M, Montecucco C. Neurotoxins affecting neuroexocytosis. Physiological Reviews 2000;80:717–766. [PubMed: 10747206]
- 36. Gouet P, Courcelle E, Stuart DI, Metoz F. ESPript: analysis of multiple sequence alignments in PostScript. Bioinformatics 1999;15:305–308. [PubMed: 10320398]



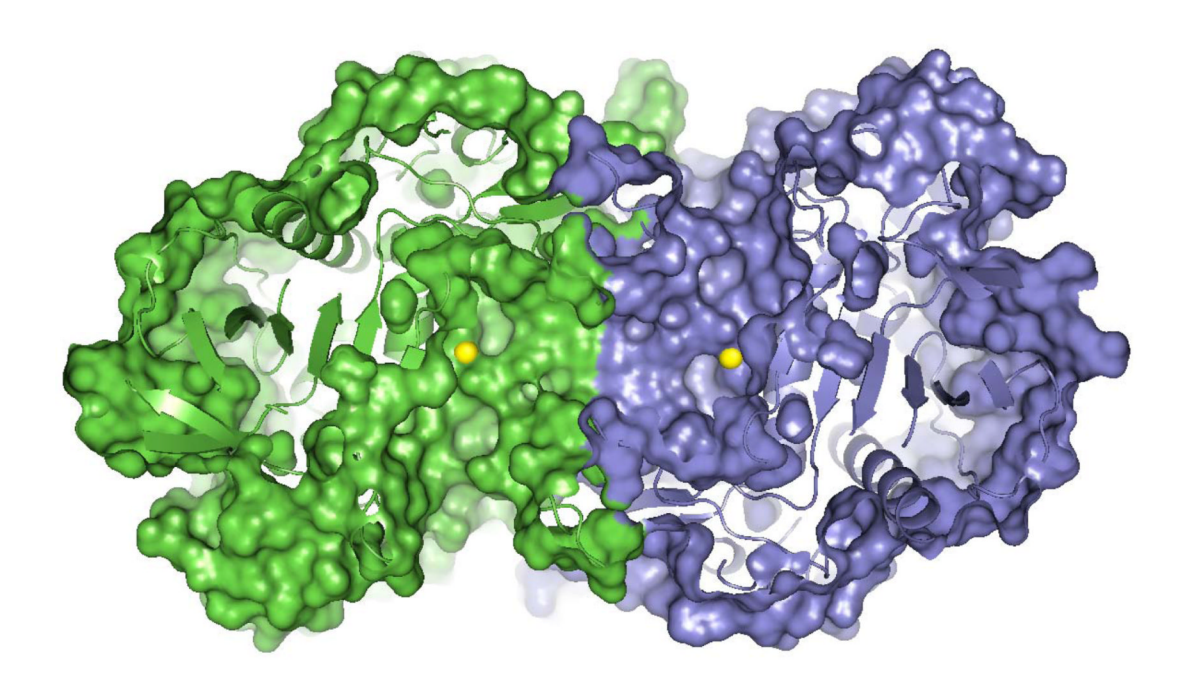


Figure 1. Crystal structure of BoNT/G-LC homodimer. (A) Ribbon diagram of *C. botulinum* BoNT/G-LC with one monomer of the crystallographic dimer colored green and the second monomer in slate blue with N- and C-terminus indicated. β -strands ($\beta 1 - \beta 14$) and α -helixes ($\alpha 1 - \alpha 8$) of one of the monomers are labeled. The active site zinc ion is shown as a yellow sphere. (B) Same as A, but a cross section of the molecular surface BoNT/G-LC homodimer overlaid with ribbons diagram looking down onto the serpentine channel that connects the two active sites.

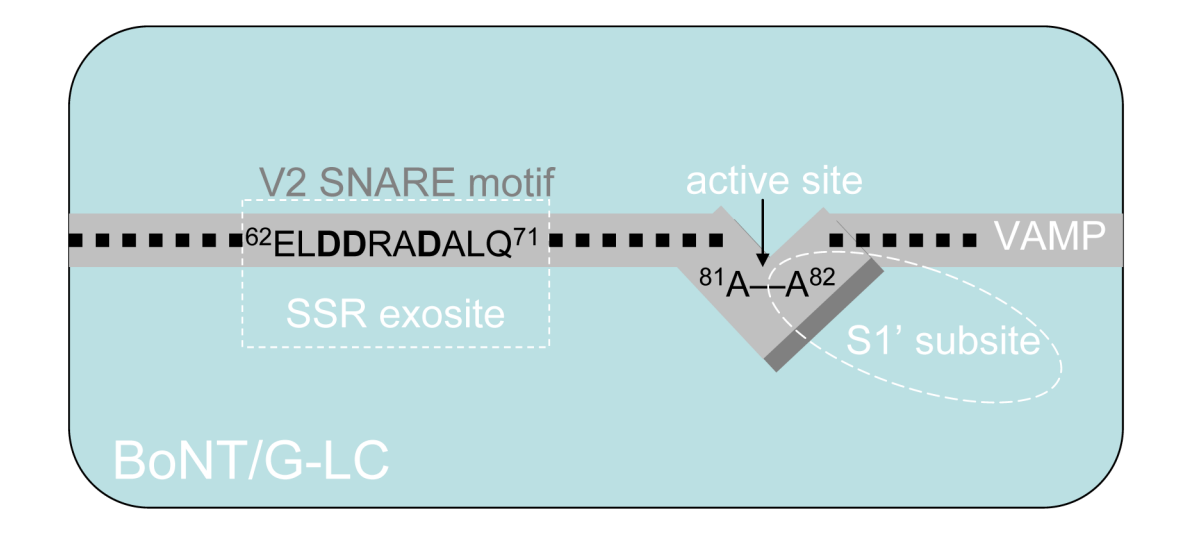


Figure 2. Schematic of the proposed interaction of BoNT/G-LC (light blue) and VAMP (gray) with S1' subsite and SSR exosite indicated. The cleavage site is identified with the arrow and essential acidic residues of the V2 SSR are in bold.

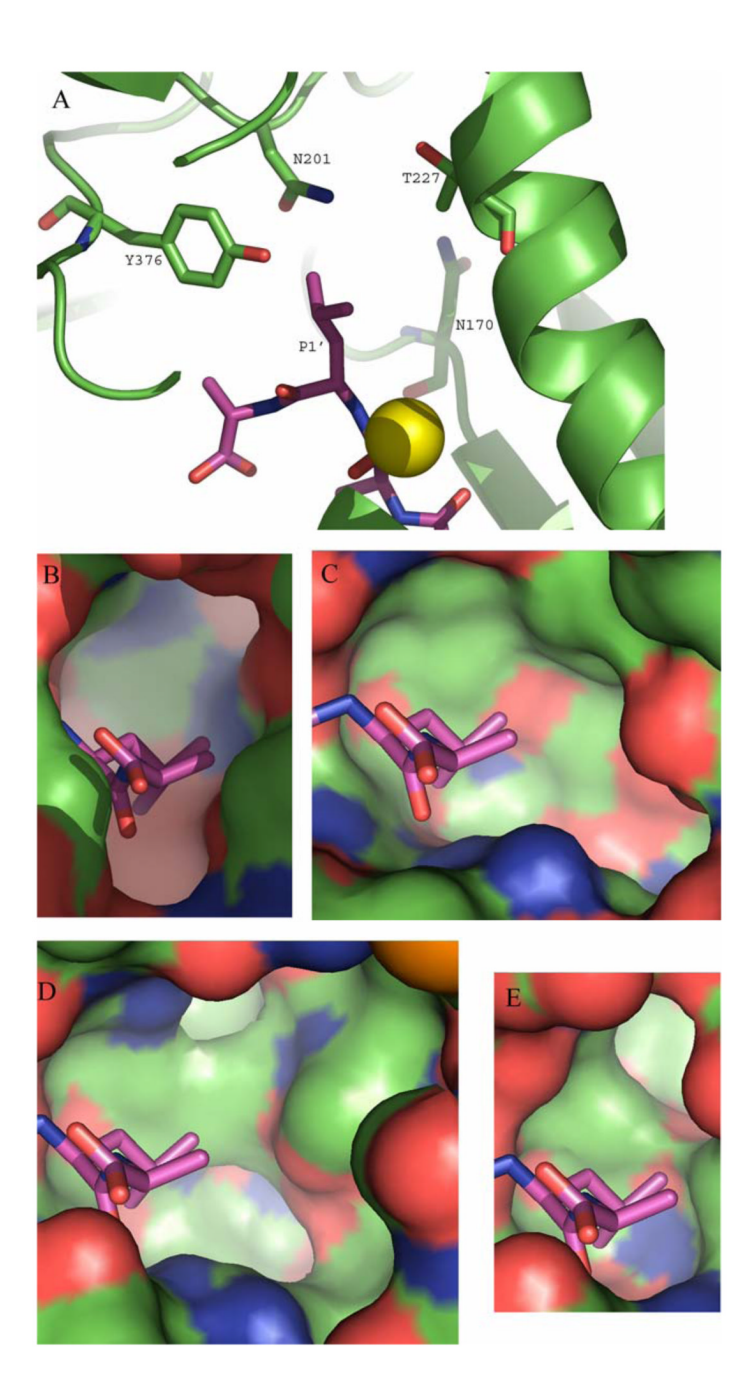


Figure 3.

(A) Close up view of putative S1' subsite of BoNT/G-LC with a modeled thermolysin transition state analog (TSA). Putative S1'-binding site residues as observed in BoNT/G-LC (green) with a modeled thermolysin TSA (violet) with residue labels and substrate P1' residue indicated. (B) Same as A, but a surface diagram looking down onto the S1' subsite of BoNT/G-LC (green) with oxygens (red) and nitrogens (blue) with a modeled TSA (magneta). (C) Same as C, but of the S1' subsite of BoNT/A1-LC (9) with the C-terminal His-tag not shown for clarity. (D) Same as C, but of the S1' subsite of BoNT/B-LC (8). (E) Same as C, but of the S1' subsite of BoNT/E-LC (23).

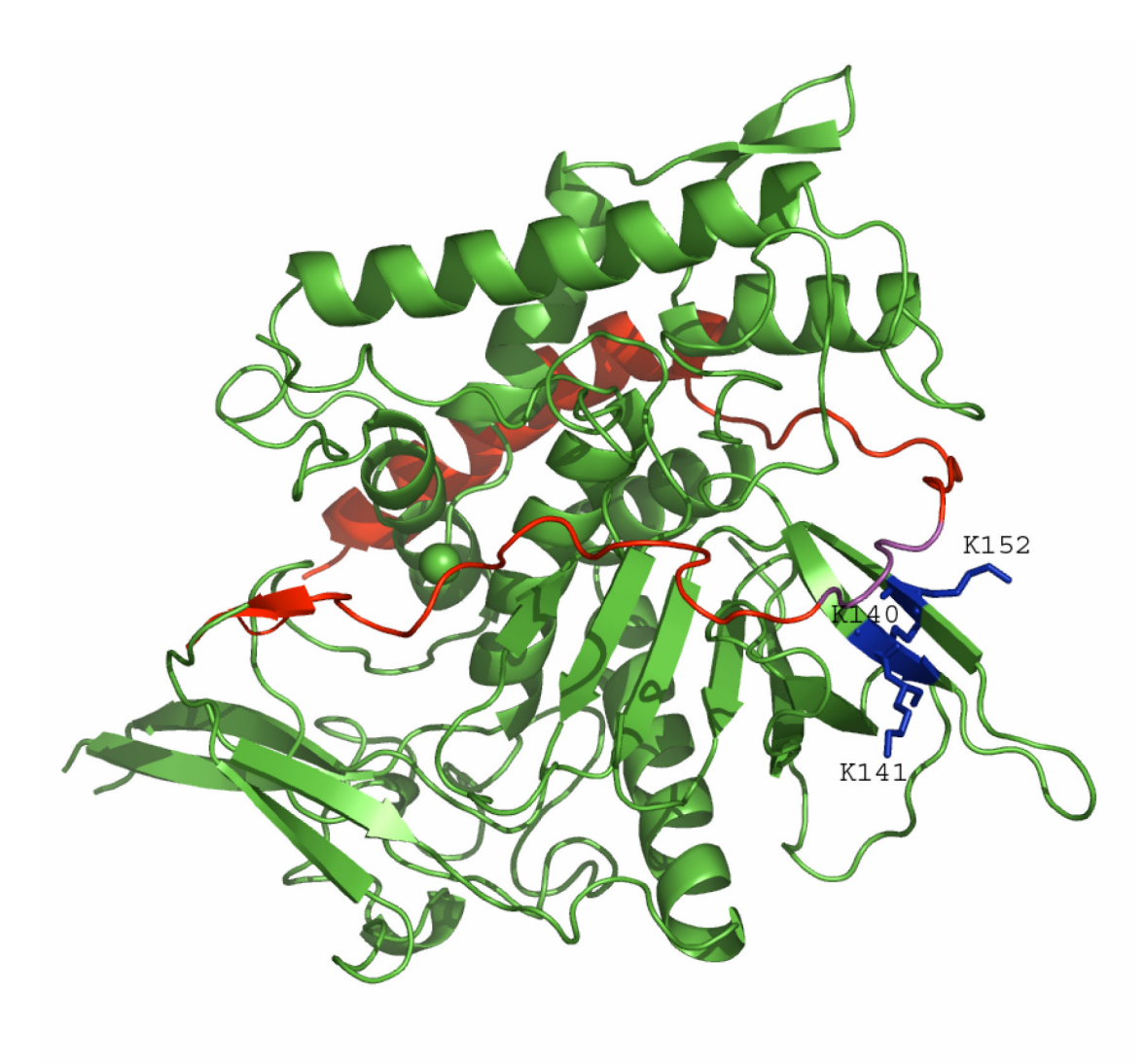


Figure 4.Putative SSR motif recognition exosite of BoNT/G-LC. Ribbons diagram of BoNT/G-LC (green) superimposed SNAP-25 (red), the substrate of BoNT/A. Basic residues in the putative BoNT/GLC exosite involved in SSR motif recognition are colored (blue) and essential substrate residues 64–68 corresponding to the V2 SSR motif of VAMP are highlighted (violet).

 Table 1

 Summary of crystallographic parameters, data collection and refinement statistics for BoNT/G-LC (PDB: 1ZB7)

Building of Crystallogic	ipine parameters, data concett
Data Collection	
Space group	P6 ₂ 22
Unit cell parameters	a = 179 Å, b = 179 Å, c = 81 Å
Resolution range (Å)	50.00 - 2.35
Highest resolution shell (Å)	2.43 - 2.35
Number of observations	225,818
Number of reflections	30,233
Completeness (%)	93.9 (96.0) +
Mean I/σ(I)	24.4 (4.8) ⁺
R _{svm} on I	$0.053(0.395)^{+}$
Model and refinement statis	tics
Resolution range (Å)	24.81 – 2.35
No. of reflections (total)	30,226
No. of reflections (test)	1,536
Completeness (% total)	94.0
R _{crvst} / R _{free}	0.174 / 0.222
Stereochemical parameters	
Restraints (RMS observed)	
Bond length	0.027 Å
Bond angle	2.03°
Protein residues / atoms	407 / 3324
Solvent molecules	197
Heterogen atoms	14

⁺highest resolution shell

 $R_{SYM} = \Sigma |I_i - \!\!<\! I_i > \mid /\!\! \sum |I_i| \text{ where } I_i \text{ is the scaled intensity of the ith measurement, and } <\! I_i > \text{ is the mean intensity for that reflection.}$

 $R_{cryst} = \Sigma |\ |F_{obs}| - |F_{calc}|\ |/\Sigma|F_{obs}| \ \ \text{where}\ F_{calc} \ \ \text{and}\ F_{obs} \ \ \text{are the calculated and observed structure factor amplitudes, respectively.}$

 $R_{free} = {\rm as\ for\ } R_{CTYSt}, \ but\ for\ 5.0\%\ of\ the\ total\ reflections\ chosen\ at\ random\ and\ omitted\ from\ refinement.$

Arndt et al.

Table 2

Summary of BoNT-LC crystal structures.

LC type	PDB	resolution (Å)	truncation construct a	C-terminus disorder	oligomeric state
A1 (9)	1XTF	2.2	ΔC18	none	monomer
A2 (22)	$_{1 \to 1 H}^{b}$	1.8	AN8 & AC32	none	dimer
B (8)	1F82	2.2	ΔC19	none	monomer
E (23)	1T3A	2.1	full length	residues 1–10	dimer
	17B7	235	full length	5_1 senbiser	dimer

 a All LCs contain C-terminal His-tags.

 b Contains 47 additional N-terminal residues consisting of His- and S-tags and a protease cleavage site.

Page 15

Table 3

	Residues composing the putative S1' subsite of BoNTs with their SNARE substrates.	e of BoN	rs with the	ir SNARI	3 substrates	٠.
NT Serotype	Substrate: cleavage point a P3-P2-P1—P1'-P2'-P3'	I	Probable residues of the S1' recognition sit	f the S1' reco	gnition site	
A	SNAP-25: ¹⁹⁵ A-N-Q— R -A-T ²⁰⁰	F163	F194	T220	D370	
В	VAMP.S-A-T-F-F-P-199	N169	8200	1226	8376	

^aP1' residue indicated in bold.

Page 16